Supporting Information

van der Vinne et al. 10.1073/pnas.1712324115

SI Materials and Methods

Animals. All animal procedures were reviewed and approved by the Institutional Animal Care and Use Committee of the University of Massachusetts Medical School (Protocol A-1315) or Williams College (Protocol SS-N-14).

All genotypes used in this study were created by crossing mice with previously described mutations. *Vgat-Cre*$^{+}$ mice with a cassette containing the Cre-recombinase coding sequence preceded by an internal ribosomal-entry sequence just downstream of the Vgat-gene stop codon (1) were kindly provided by Bradford B. Lowell, Beth Israel Deaconess Hospital, Harvard Medical School, Boston. Generation of mice with *LoxP* sites flanking exon 2 of *CK1δ* (JAX stock no. 10487) or exons 2 and 3 of *CK1ε* (JAX stock no. 10489) was described previously (2). PER2::LUC mice with an in-frame fusion of firefly luciferase to PER2, and an SV40 polyadenylation signal (3) were generously provided by Joseph S. Takahashi, University of Texas Southwestern Medical School, Dallas. All lines used in the study were backcrossed to C57BL/6J mice obtained from Jackson Laboratories. Whenever possible, Cre-positive and Cre-negative littermates were included in experiments to allow within-litter comparisons between genotypes.

Unless otherwise specified, mice were group housed (≤5 mice per cage) in single-sex groups in our breeding facility 12-h light/12-h dark lighting cycle, 22 ± 1 °C). Mice had access to ad libitum water and food (Prolab Isopro RMH 3000; LabDiet) unless otherwise specified. Pups were weaned ∼21–23 d of age and housed in single-sex groups. Genotyping from ear biopsies was performed using PCR-based methods as described previously (1, 2, 4).

Statistical Comparisons. All statistical tests were performed using restricted maximum-likelihood mixed models (α = 0.05) in SAS JMP 7.0 for Windows unless indicated otherwise. Animal identification (ID) was included as a random independent variable in analyses where repeated measurements were performed on the same individual. When categorical variables with more than two categories revealed statistical significant differences, Tukey HSD post hoc tests were performed. Data are represented as mean ± SEM. Both male and female mice were used in all experiments. Sex did not influence any of the assessed circadian characteristics (Fig. S1*A*) and was therefore excluded from the statistical analyses of these parameters. For structural and metabolic endpoints, the effect of sex on the variable of interest was assessed statistically (e.g., genotype × sex or genotype × age × sex), and data corrected for the main effect of sex is reported when this interaction was not significantly altered by sex. Data are reported separately for both sexes in supplemental figures. Presented statistical outcomes represent the main effect of genotype unless specified otherwise.

Circadian Characteristics of Mice. The circadian period of behavioral activity was assessed in different *CK1δ*/*ε* genotypes. Mice were transferred to our experimental room and single housed in running-wheel cages. Running-wheel activity was monitored by detecting magnetic switch closures from magnets attached to the running wheel, detected using ClockLab collection software. Mice were exposed to a 12-h light/12-h dark lighting cycle for 10 d, followed by 20 d in constant darkness. Free-running period was determined by periodogram analysis between day 10 and 20 of constant darkness (5). Because the genotype influence on period was similar in both sexes (sex × genotype: $F_{5,145} = 1.507$; $P = 0.1913$), the effect of genotype on period was assessed in a general linear model with only genotype and sex as dependent variables. Sample size per genotype and sex is indicated at the base of bars in Fig. S1*A*.

PER2::LUC bioluminescence measurements of SCN, pituitary, lung, and liver tissue explants were performed as described previously (4, 6). Tissues were collected from animals housed in a 12-h light/12-h dark lighting cycle in our breeding colony. Mice were deeply anesthetized with ketamine/xylazine (Ketaved; Vedco; Rompun; Bayer) or euthasol (Virbac AH) and then decapitated. Tissues were quickly removed and placed in ice-cold HBSS. Coronal 350-μm brain slices were made using a vibratome. SCN-containing sections were identified based on anatomical landmarks and SCN explants were obtained using scalpel blade cuts. The anterior pituitary was subdivided into four sections that were cultured individually. Three to six lung or liver explants (∼2 mm^3) were cultured together per dish, with up to three culture dishes per animal. Explants were cultured in "air" recording medium (4) on sterile 35-mm Millicell culture plate inserts (Millicell PICM ORG 50; Millipore) in an air-sealed petri dish. Culturing was performed at 37 °C for SCN [sample size: *Vgat-Cre*$^{+}$ *CK1δ*$^{fl/fl}$: 5 males (M), 7 females (F); *Vgat-Cre*$^{+}$ *CK1ε*$^{fl/fl}$: 3 M, 6 F; *Vgat-Cre*$^{+}$ *CK1δ*$^{fl/+}$ *ε*$^{fl/fl}$: 7 M, 4 F; *Vgat-Cre*$^{+}$ *CK1δ*$^{fl/fl}$ *ε*$^{fl/+}$: 8 M, 6 F; *No-Cre CK1δ*$^{fl/fl}$ *ε*$^{fl/+}$: 14 M, 6 F], pituitary (sample size: *Vgat-Cre*$^{+}$ *CK1δ*$^{fl/fl}$: 4 M, 6 F; *Vgat-Cre*$^{+}$ *CK1ε*$^{fl/fl}$: 2 M, 9 F; *Vgat-Cre*$^{+}$ *CK1δ*$^{fl/+}$ *ε*$^{fl/fl}$: 5 M, 3 F; *Vgat-Cre*$^{+}$ *CK1δ*$^{fl/fl}$ *ε*$^{fl/+}$: 4 M, 7 F; *No-Cre CK1δ*$^{fl/fl}$ *ε*$^{fl/+}$: 8 M, 2 F) and lung (sample size: *Vgat-Cre*$^{+}$ *CK1δ*$^{fl/fl}$: 10 M, 9 F; *Vgat-Cre*$^{+}$ *CK1ε*$^{fl/fl}$: 2 M, 4 F; *Vgat-Cre*$^{+}$ *CK1δ*$^{fl/+}$ *ε*$^{fl/fl}$: 5 M, 5 F; *Vgat-Cre*$^{+}$ *CK1δ*$^{fl/fl}$ *ε*$^{fl/+}$: 11 M, 13 F; *No-Cre CK1δ*$^{fl/fl}$ *ε*$^{fl/+}$: 13 M, 5 F) samples. Liver samples (sample size: *Vgat-Cre*$^{+}$ *CK1δ*$^{fl/fl}$ *ε*$^{fl/+}$: 5 M, 2 F; *No-Cre CK1δ*$^{fl/fl}$ *ε*$^{fl/+}$: 2 M, 4 F) were cultured at 32.5 °C to increase viability with lung samples from the same mice measured simultaneously as a control. PER2::LUC bioluminescence was measured for 1 min every 15 min on a Hamamatsu LM-2400 luminometer for at least 3 d. The first 12 h of data were discarded to prevent acute culturing-related artifacts from influencing assessment of rhythms. Photon counts were smoothed using a 3-h running average and baseline subtracted by a running average with a period similar to the average genotype's period of the assessed tissue. The circadian period of PER2::LUC bioluminescence of each culture was calculated by averaging the periods derived by two separate linear regressions of all upward and all downward crossings through zero observed in the smoothed detrended data between 24 and 60 h after the start of the bioluminescence recording. Statistical comparisons of period differences between genotypes were made for each tissue using mixed models with animal ID included as a random variable to account for animals in which replicates of the same tissue were measured.

Phase-response curves of mice of three genotypes (*Vgat-Cre*$^{+}$: 15 M, 5 F; *Vgat-Cre*$^{+}$ *CK1δ*$^{fl/+}$ *ε*$^{fl/fl}$: 16 M, 4 F; and *Vgat-Cre*$^{+}$ *CK1δ*$^{fl/fl}$ *ε*$^{fl/+}$: 16 M, 5 F) were determined based on behavioral phase shifts in response to light pulses. Mice were single-housed in running-wheel cages for multiple weeks and exposed repeatedly to a 1-h light pulse at a random time of day (2–9 light pulses per animal) with at least 9 d between light pulses. The phase shift in hours and the internal circadian time during the light exposure were determined for each light pulse based on the timing of activity onsets. Cumulatively, the response to a total of 132–152 light exposures was determined in 20–21 animals per genotype. Differences in phase responses between genotypes were assessed in a mixed model with genotype, circadian time as a categorical variable with 2-h intervals, and animal ID as a random factor.

The range of entrainment of Discordant (5 M, 5 F) and Cre-negative control (4 M, 4 F) mice was determined by exposing

single-housed mice with access to a running wheel to T-cycles with different durations. Mice raised in a 12-h light/12-h dark lighting cycle were exposed to T-cycles with the light portion (150–400 lx) representing half of the T-cycle length. T-cycles were adjusted in 1-h steps between 23 and 28 h after 14 cycles on each cycle length, with half of the mice on a lengthening and half on a shortening schedule. Whether a mouse was entrained to a T-cycle was scored based on visual inspection of actograms plotted at the frequency of the T-cycle (Fig. S1*D*).

In Vivo Peripheral PER2::LUC Rhythms. Procedures for in vivo measurement of PER2::LUC bioluminescence rhythms were adapted from ref. 7. Discordant and Cre-negative control mice were individually housed in running-wheel cages for 12–13 d in constant darkness (Fig. 2; *Vgat-Cre*$^{+}$ *CK1δ*$^{fl/fl}$ *ε*$^{fl/+}$: 2 M, 6 F; *No-Cre CK1δ*$^{fl/fl}$ *ε*$^{fl/+}$: 3 M, 6 F) or for 61 d in a 2-h light/23.5-h dark (25.5 h T-cycle; *Vgat-Cre*$^{+}$ *CK1δ*$^{fl/fl}$ *ε*$^{fl/+}$: 4 M, 2 F; *No-Cre CK1δ*$^{fl/fl}$ *ε*$^{fl/+}$: 4 M, 3 F) lighting cycle (Fig. 6). Mice were moved in a light-tight box to the measurement room 3 h (constant darkness) or 14 h (25.5-h T-cycle) before the first measurement. All procedures were performed in darkness except for a handheld dim red light unless procedures occurred during the light phase. Shaving of dorsal and ventral fur was performed under anesthesia in the hour preceding the first measurement. For each of 5–7 measurements taken over a 24- to 30-h interval, mice were anesthetized (2% isoflurane; Zoetis Inc.) and injected i.p. with 0.25 mg Luciferin in 0.1 mL saline solution (D-Luciferin potassium salt; Gold Biotechnology). Dorsal (9 min postinjection) and ventral (10.5 min postinjection) images were taken using the IVIS-100 system (10 s integration; Xenogen Imaging Technologies) of the University of Massachusetts Medical School Small Animal Imaging Core Facility. The circadian time of measurements was determined based on extrapolation of activity onsets, performed independently by two experienced investigators. To compare the same anatomical area across time points, the size and shape of the region of interest (ROI) was determined in the image with highest PER2::LUC bioluminescence, and this ROI was used to quantify all five or six time points (Caliper LifeSciences Living Image software v4.4). A cosinor curve with a period identical to that of the behavioral rhythm was fitted (MS Excel Solver function) to data from each organ to determine the relative phase relationship between the timing of activity and PER2::LUC bioluminescence rhythms as well as the relative amplitude (cosinor amplitude/cosinor average) of each peripheral organ. The suitability of using a cosinor analysis to describe peripheral in vivo PER2::LUC bioluminescence rhythms was confirmed by plotting the relative residuals versus the circadian time of measurements (Fig. S2*C*) and calculating the goodness of fit of the cosinor fits (Fig. S2*B*). The absence of a correlation between the first measurement's circadian time and observed peak phase of PER2::LUC bioluminescence (Fig. S2*D*) shows that in vivo PER2::LUC bioluminescence rhythms were not synchronized by the measurement procedure. Peak-phase estimates derived from the cosinor analyses were used to determine whether organs of both genotypes were entrained with a period of 24 circadian hours (phase clustering; Rayleigh test) and whether the entrained phase was different between genotypes (Watson U^2 test).

Body Temperature and Energy Expenditure. Discordant (6 M, 6 F) and Cre-negative control (6 M, 7 F) mice were implanted i.p. with a telemeter to measure locomotor activity and body temperature (TA-F10; Data Sciences International) as previously described (8). Anesthesia was initiated with 5% isoflurane in a 100% oxygen stream, followed by 2% isoflurane during the rest of the procedure. Mice were provided with ad libitum food (D12450B; Research Diets Inc.) and water throughout the experiment. Individually housed mice were placed in a custom-built indirect calorimetry setup that determined energy expenditure and respiratory quotient by measuring O_2 concentration (S-3A/H O_2 analyzer; AEI Technologies), CO_2 concentration (CD-3A CO_2 analyzer; AEI Technologies), and airflow (FMA-5606; Omega) every 4 min and comparing these to measurements of a reference channel. Energy expenditure, mass-specific energy expenditure, and respiratory quotient were calculated from O_2 use and CO_2 production by the following formulas: $EE = 16.18 \times O_2 + 5.02 \times CO_2$; mass-specific EE = EE/body mass; $RQ = CO_2/O_2$. General locomotor activity and body temperature were recorded by telemeter every minute. Measurements were performed for at least 9 d in constant darkness. Circadian period and the timing of activity onsets were determined based on telemeter activity recordings and used to select a single rest–activity cycle with a duration of 24 circadian hours for each mouse. To compare between animals with different endogenous periods, measurements taken every minute (body temperature) or 4 min (energy expenditure, respiratory quotient) were converted to a similar time scale by averaging all measurements taken over an interval of 30 circadian minutes for each animal. Circadian profiles per genotype and sex were calculated by averaging body temperature, energy expenditure, mass-specific energy expenditure, or respiratory quotient at each circadian timepoint (circadian profiles in Fig. 3). Average values during the rest phase (circadian time 0–12), active phase (circadian time 12–24), and over the full circadian cycle were calculated per animal and compared between genotypes for both sexes (Fig. S3). The absolute difference between active-phase and rest-phase values was calculated per animal and used to compare differences in amplitude between genotypes in each sex.

Body Mass, Size, and Blood Glucose. Body mass of mice raised and maintained in a 12-h light/12-h dark lighting cycle was determined by weighing 100- to 150-d-old mice in our breeding colony. In view of the large sample size, data are presented separately for male and female mice (Fig. 4) even though sex did not significantly alter the genotype effect on body mass. Age was included in the statistical model as a continuous independent variable, whereas the interaction between age and genotype (age × genotype) was excluded because it did not significantly predict body mass. The body mass of a separate batch of Discordant (10 M, 9 F) and Cre-negative control (6 M, 7 F) mice was recorded at 18 mo of age to assess whether the body mass differences observed in younger mice persisted into older age.

Subsequent comparisons between Discordant mice and Cre-negative littermate controls were performed to further investigate differences in body mass, body length, and glucose tolerance between these genotypes. Study animals were generated using parents that entrain to a 12-h light/12-h dark lighting cycle (*No-Cre CK1δ*$^{fl/fl}$ *ε*$^{fl/fl}$ × *Vgat-Cre*$^{+}$ *CK1δ*$^{fl/fl}$). Dam and pups were transferred to constant darkness within 24 h of giving birth. Pups remained in constant darkness throughout their life, except for brief exposure to dim red light from handheld lights during procedures requiring investigator vision. Pups used for body mass assessment were weaned at 28 ± 2 d (mean ± SD) of age and were individually housed at 33 ± 3 d (mean ± SD) without access to a running wheel. Standardized nesting conditions were ensured by providing mice with a disposable mouse home without providing additional nesting materials. Mice not used for body mass measurements remained group housed (≤5 mice per cage) until activity monitoring was required before blood glucose measurements. Five- to 20-wk-old mice were weighed weekly (Discordant mice: 6 M, 8 F; control mice: 6 M, 8 F), and the behavioral circadian period (Fig. S4*A*) was determined by recording general locomotor activity for ∼10 d using passive infrared motion sensors connected to a registration computer using ClockLab collection software.

Glucose tolerance tests were performed when mice were 23–33 wk old (Discordant mice: 14 M, 16 F; control mice: 12 M, 16

F). Tests were performed in the middle of the rest phase (circadian time 6) as determined through general locomotor activity records. Following a 6-h fast, mice were injected i.p. with glucose solution [2.0 mg/gram body mass, D-(+)-Glucose; Sigma-Aldrich]. Blood samples were obtained by tail snipping to measure blood glucose concentration at baseline, 20, 40, 60, and 120 min post-injection (TrueTrack smart system; Nipro Diagnostics). AUC was calculated by trapezoidal method after subtraction of baseline glucose levels.

Body length (distance from nose to base of the tail) and the circadian profile of blood glucose concentration were measured in 25- to 40-wk-old mice that had been housed in running wheel cages for 3–4 wk to determine circadian time (Discordant mice: 20 M, 17 F; control mice: 20 M, 21 F). CircWave analysis was used to detect circadian rhythms in blood glucose concentration (9). Statistical comparisons between the circadian rhythms in blood glucose of both genotypes were made using a CircWave procedure in which average, amplitude, and phase were estimated simultaneously (MS Excel Solver function).

To provide an additional metabolic challenge, a second cohort of Discordant mice and their Cre-negative littermate controls were raised in constant darkness following the procedures described above but fed a high-fat diet. High-fat diet (60% fat content, D12492; Research Diets Inc.) was first provided after the first weighing session when mice were 36 ± 1 d old (mean ± SD). Body mass was measured weekly from 5 to 16 wk of age (Discordant mice: 8 M, 5 F; control mice: 8 M, 7 F). Glucose tolerance tests were performed on these mice at 15–19 wk of age (Discordant mice: 8 M, 5 F; control mice: 7 m, 7 f). Food was removed at the onset of activity, resulting in an 18 circadian-hour fasting period. Daily torpor was not observed during the glucose tolerance tests. Body length was measured in 17- to 20-wk-old mice (Discordant mice: 8 M, 5 F; control mice: 8 M, 7 F).

The phase of food intake was determined in a separate batch of Discordant (4 M, 3 F) and Cre-negative littermate controls (3 M, 4 F) by measuring the timing of feeder visits in mice housed in constant darkness. The timing of circuit closures resulting from physical contact with the feeder was measured for up to three circadian cycles. The proportion of feeder visits occurring in each two-circadian-hour bin was determined for each mouse and compared between genotypes (Fig. S4*B*).

Body mass between age 5 and 20 wk, as well as body length (age 17–32 wk), was also measured in chow-fed *Vgat-Cre*$^{+}$ *CK1δ*$^{fl/+}$ *ε*$^{fl/fl}$ mice (8 M, 8 F) and their No-Cre littermate controls (8 M, 8 F) using the methods described above for Discordant mice (Fig. S7).

All statistical models of mice raised in constant darkness included litter as a random variable to allow within-litter comparisons between genotypes.

The lower body mass of Discordant mice dictated that they received a lower amount of glucose during glucose tolerance tests. To make sure that glucose tolerance test results were not influenced by the lower dose of glucose injected into Discordant mice, a separate group of chow-fed wild-type mice (12 F) housed in a 12-h light/12-h dark lighting cycle was tested on two consecutive weeks using different amounts of glucose (Fig. S4*D*). Glucose amounts were either 90 or 100% of the regular glucose dose (2.0 mg/gram body mass) and tests were performed in the middle of the light phase (Zeitgeber time 6–7) following a 6-h fast. The order in which mice received the dosages was balanced between treatments.

Reducing Internal Desynchrony. To test whether body mass differences between Discordant and Cre-negative control mice were caused by internal desynchrony or unrelated pleiotropic effects, a separate cohort of Discordant and Cre-negative littermates was entrained to a 2-h light/23.5-h dark lighting cycle. This procedure was intended to reduce internal desynchrony in the Discordant mice and generate a comparable level of internal desynchrony in the two genotypes. Procedures were similar to those described above for Discordant mice studied in constant darkness. General locomotor activity was recorded by passive infrared motion detectors throughout the experiment to confirm entrainment to the 25.5 h T-cycle, resulting in the exclusion of one Discordant mouse from analyses because of a lack of entrainment. Body mass was measured between 5 and 20 wk of age (Discordant mice: 4 M, 5 F; control mice: 7 M, 9 F). Glucose tolerance was measured in 19- to 26-wk-old mice (Discordant mice: 3 M, 4 F; control mice: 6 M, 5 F), and body length was recorded at age 24–37 wk (Discordant mice: 2 M, 4 F; control mice: 7 M, 9 F). The effect of correcting internal desynchrony was assessed by comparing results in the 25.5-h T-cycle to results obtained in constant darkness. Statistically, this was done by testing the interaction between lighting condition with the variable of interest (lighting condition × genotype or lighting condition × genotype × age), while including litter as a random variable to allow within-litter comparisons of the genotype effect.

1. Vong L, et al. (2011) Leptin action on GABAergic neurons prevents obesity and reduces inhibitory tone to POMC neurons. *Neuron* 71:142–154.
2. Etchegaray JP, et al. (2009) Casein kinase 1 delta regulates the pace of the mammalian circadian clock. *Mol Cell Biol* 29:3853–3866.
3. Welsh DK, Yoo SH, Liu AC, Takahashi JS, Kay SA (2004) Bioluminescence imaging of individual fibroblasts reveals persistent, independently phased circadian rhythms of clock gene expression. *Curr Biol* 14:2289–2295.
4. Yoo SH, et al. (2004) PERIOD2:LUCIFERASE real-time reporting of circadian dynamics reveals persistent circadian oscillations in mouse peripheral tissues. *Proc Natl Acad Sci USA* 101:5339–5346.
5. Schmid B, Helfrich-Förster C, Yoshii T (2011) A new ImageJ plug-in "ActogramJ" for chronobiological analyses. *J Biol Rhythms* 26:464–467.
6. DeBruyne JP, Weaver DR, Reppert SM (2007) Peripheral circadian oscillators require CLOCK. *Curr Biol* 17:R538–R539.
7. Tahara Y, et al. (2012) *In vivo* monitoring of peripheral circadian clocks in the mouse. *Curr Biol* 22:1029–1034.
8. Chu LP, Swoap SJ (2012) Oral bezafibrate induces daily torpor and FGF21 in mice in a PPAR alpha dependent manner. *J Therm Biol* 37:291–296.
9. Oster H, Damerow S, Hut RA, Eichele G (2006) Transcriptional profiling in the adrenal gland reveals circadian regulation of hormone biosynthesis genes and nucleosome assembly genes. *J Biol Rhythms* 21:350–361.

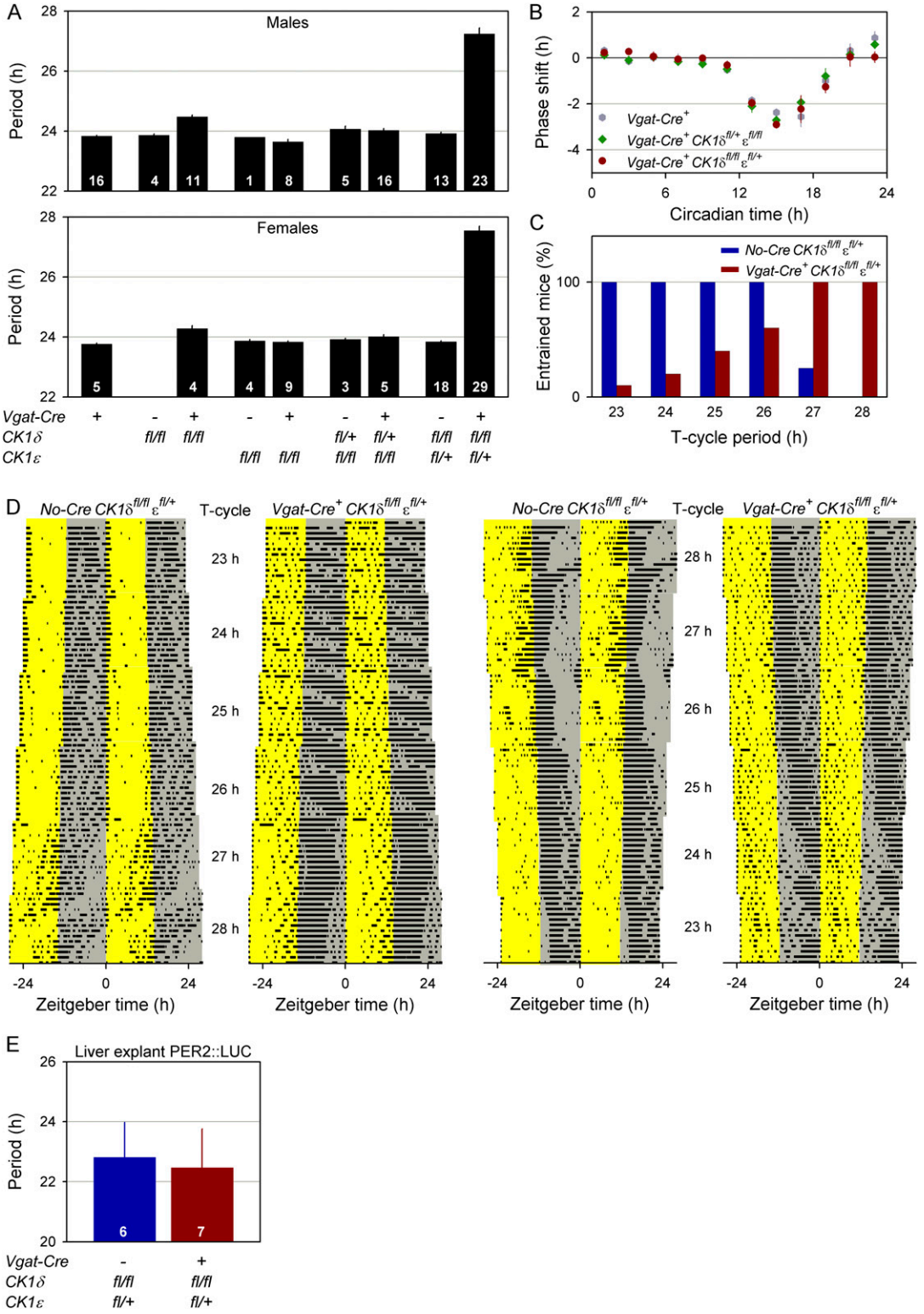

Fig. S1. Discordant mice have slow but robust circadian clocks. (*A*) Behavioral period of different *Vgat-Cre CK1δ/ε* genotypes in male (*Upper*) and female mice (*Lower*). Bar graphs are mean ± SEM. Sample size per genotype is indicated at the base of each bar. (*B*) Phase response curves reveal no significant genotype differences in phase shifting following 1-h light pulses. Data are represented as mean ± SEM. (*C*) Percentage of Discordant (*Vgat-Cre*$^{+}$ *CK1δ*$^{fl/fl}$ *ε*$^{fl/+}$; $n = 10$) and Cre-negative control (*No-Cre CK1δ*$^{fl/fl}$ *ε*$^{fl/+}$; $n = 8$) mice entrained to lighting cycles of different length (T-cycle). (*D*) Representative double-plotted wheel-running actograms of the range-of-entrainment experiment presented in *C*. Mice were exposed to lengthening (23 h → 28 h; *Left*) or shortening (28 h → 23 h; *Right*) T-cycles, with each T-cycle being repeated for 14 lighting cycles. Data are plotted with the frequency of the tested T-cycle to ease the assessment of entrainment state. Irrespective of the direction of T-cycle changes, Discordant mice entrain to long (27–28 h) but not to short (23–24 h) T-cycles, whereas this pattern is inverted in Cre-negative control mice. The light and dark phases are indicated by the yellow and gray background, respectively. (*E*) Liver explant PER2::LUC bioluminescence period comparison of Discordant and Cre-negative control mice recorded at 32.5 °C. The short period of PER2::LUC rhythms in liver explants was likely a consequence of the lowered ambient temperature, because similar period lengths were seen in lung explants cultured in parallel. Bar graphs are mean ± SEM. Sample size per genotype is indicated at the base of each bar.

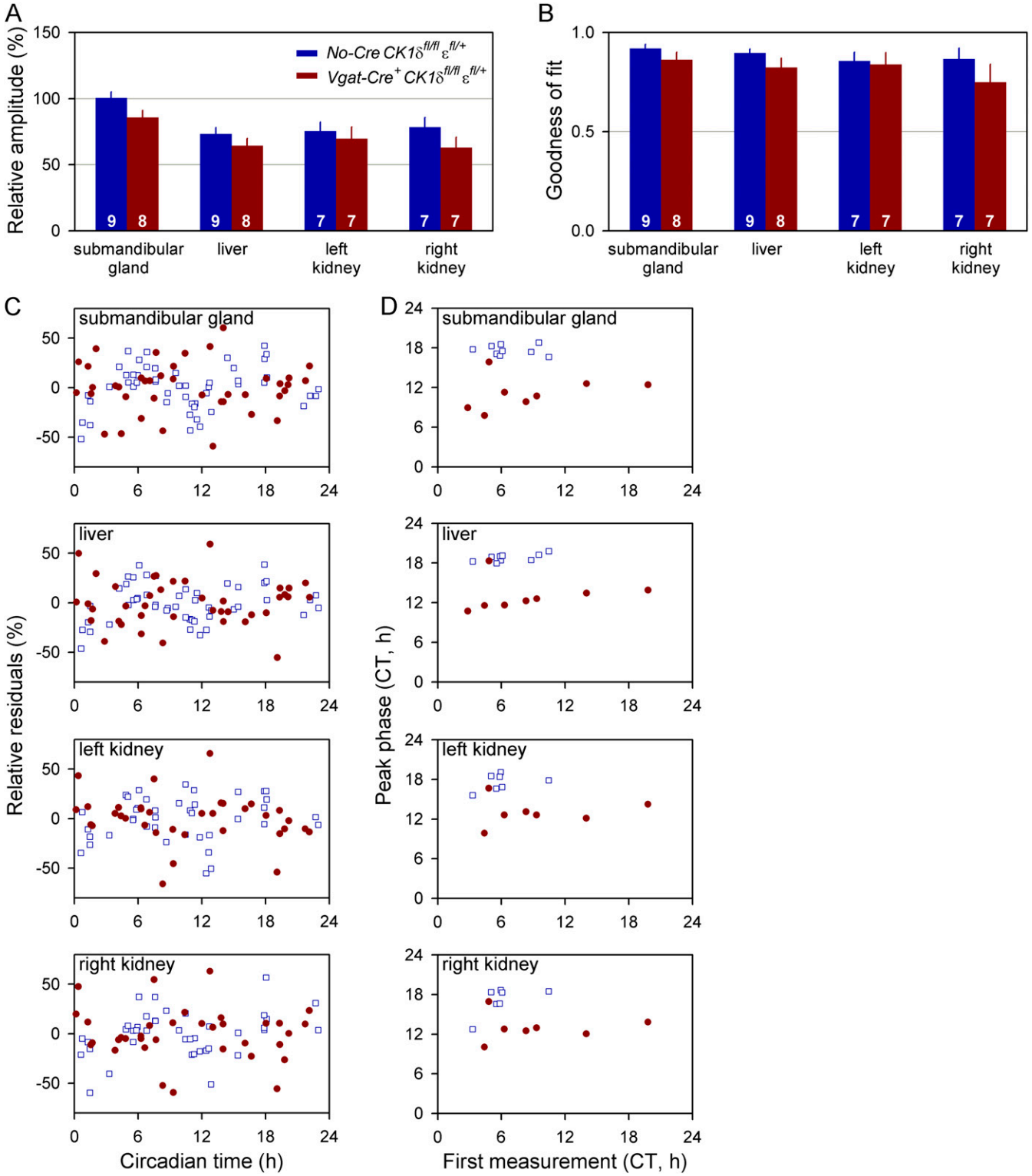

Fig. S2. In vivo measurement of peripheral PER2::LUC bioluminescence. (*A*) Relative amplitude (cosinor amplitude/cosinor average) comparison of Discordant (*Vgat-Cre*$^{+}$ *CK1*$\delta^{fl/fl}$ $\varepsilon^{fl/+}$ *Per2::Luc/+*) and Cre-negative control (*No-Cre CK1*$\delta^{fl/fl}$ $\varepsilon^{fl/+}$ *Per2::Luc/+*) mice for different peripheral tissues. No significant genotype differences were observed. (*B*) Goodness of fit of the cosinor fits used to assess rhythmicity of in vivo PER2::LUC bioluminescence measurements. No significant differences in goodness of fit were observed between genotypes. The high goodness of fit shows that a cosinor fit provides a good description of the data. (*C*) Relative residuals (residual/cosinor average) versus circadian time of each measurement for different peripheral organs. The absence of a consistent pattern suggests that a cosinor fit has an appropriate waveform to assess rhythmicity of in vivo PER2::LUC bioluminescence measurements. (*D*) Timing of peak PER2::LUC bioluminescence derived from cosinor analysis versus the time of the first PER2::LUC bioluminescence measurement. The absence of a relationship with a slope of 1 between these variables shows that the observed PER2::LUC bioluminescence peak phase in these tissues is independent of the start time of the imaging procedure. Bar graphs are mean ± SEM. Sample size is indicated at the base of each bar; incomplete shaving resulted in reduced sample sizes for kidney measurements.

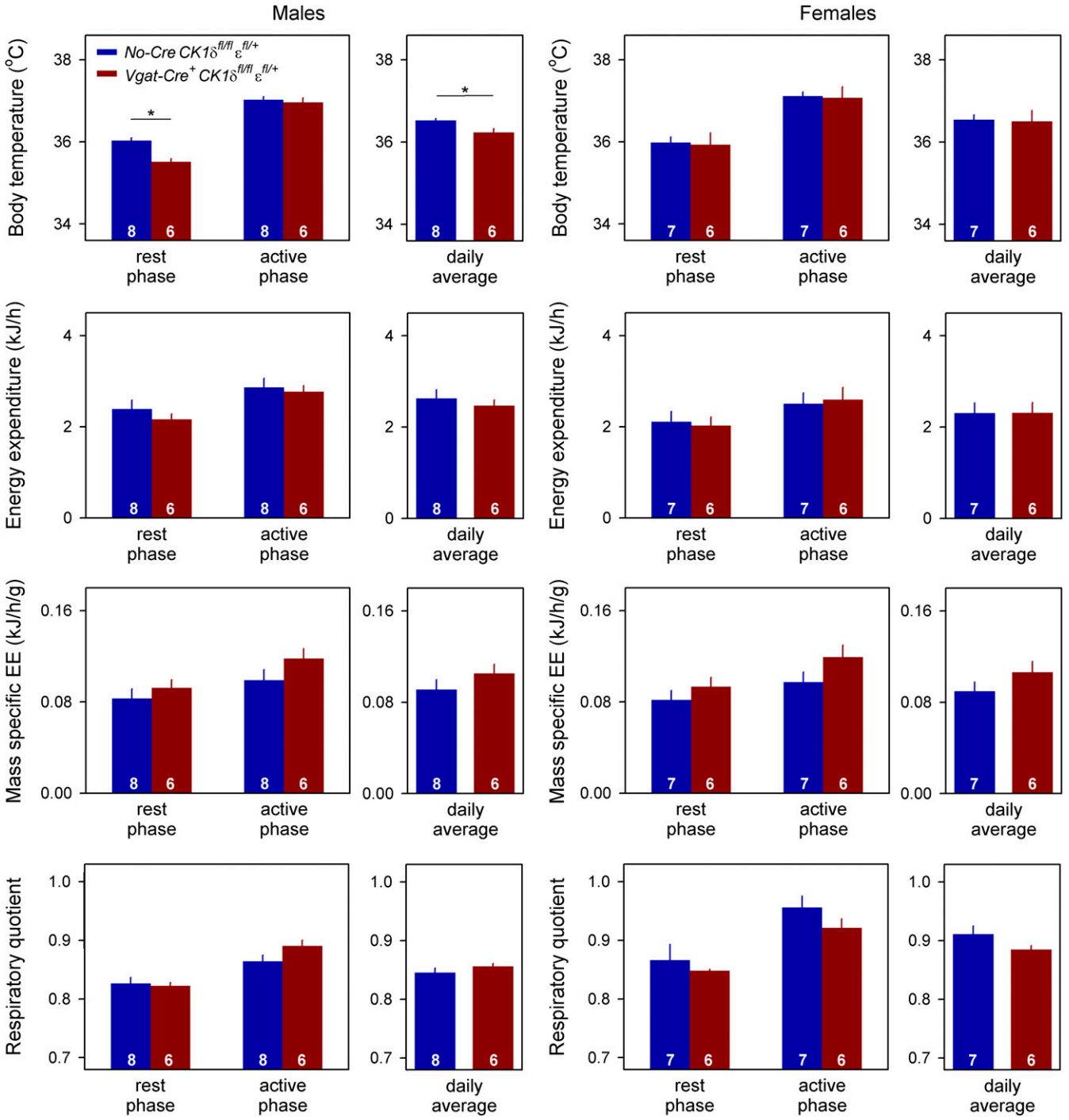

Fig. S3. Quantification of body temperature, energy expenditure, and respiratory quotient in male and female mice. Body temperature, energy expenditure, and respiratory quotient were measured for a single full rest–activity cycle of Discordant (*Vgat-Cre*$^{+}$ *CK1δ*$^{fl/fl}$ *ε*$^{fl/+}$) and Cre-negative control (*No-Cre CK1δ*$^{fl/fl}$ *ε*$^{fl/+}$) mice housed in constant darkness. Period and phase were determined based on general locomotor activity onsets. By definition, circadian time 12 corresponds to activity onset, and a single rest–activity cycle lasts 24 circadian hours. The rest phase is defined as circadian time 0–12, and the active phase is between circadian time 12 and 24. Average body temperature, energy expenditure, mass-specific energy expenditure (EE), and respiratory quotient values throughout the rest phase, active phase, and full circadian cycle are presented for male and female mice separately. Bar graphs are mean ± SEM. Sample size per genotype is indicated at the base of each bar. Asterisks indicate significant differences between genotypes.

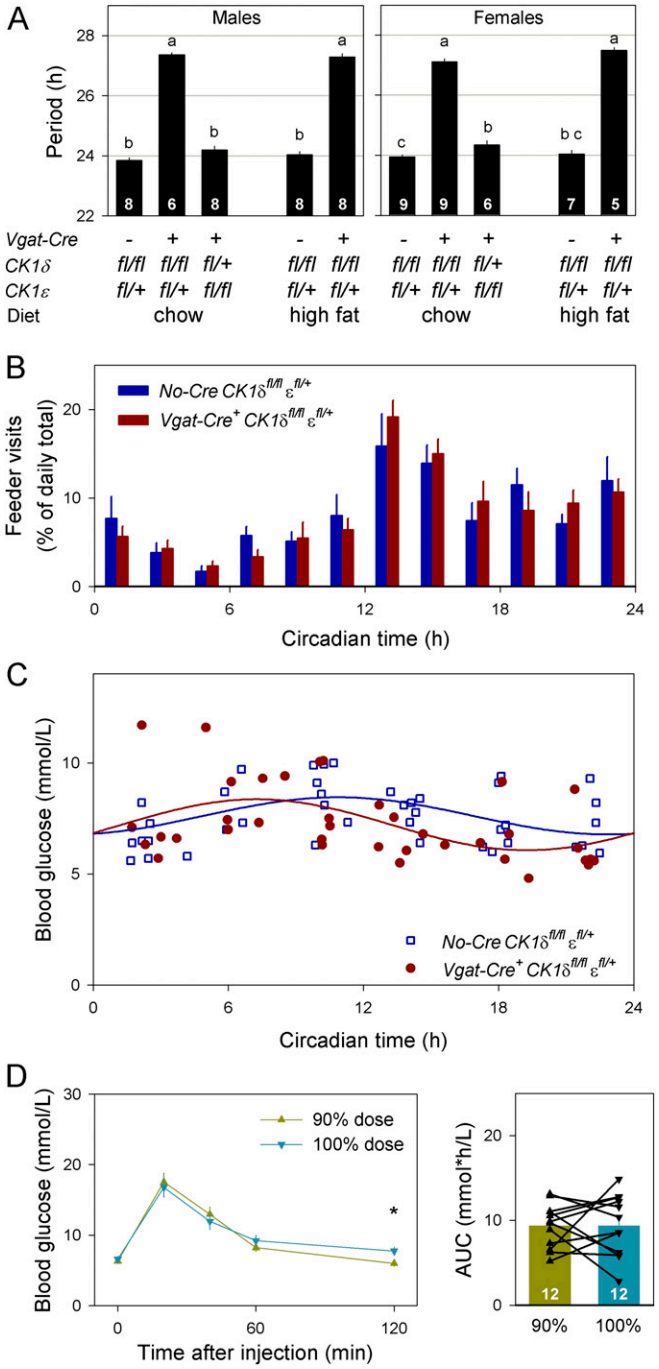

Fig. S4. Supporting data related to experiments assessing the effects of internal desynchrony in constant darkness. (*A*) Period comparisons of *Vgat-Cre CK1δ/ε* genotypes on chow- or high-fat diet in male and female mice raised in constant darkness. Locomotor behavior was measured using passive infrared detectors in adolescent mice (40–80 d old), and period was determined by periodogram analysis. The period difference between Discordant and other genotypes was not altered by early life exposure to lighting cycles or high-fat diet. Genotypes identified with different letters are significantly different. (*B*) Circadian rhythm in feeder visits of Discordant (*Vgat-Cre*$^{+}$ *CK1δ*$^{fl/fl}$ *ε*$^{fl/+}$) and Cre-negative control (*No-Cre CK1δ*$^{fl/fl}$ *ε*$^{fl/+}$) mice housed in constant darkness. No significant genotype difference in circadian rhythm of feeder visits was observed (genotype × time: $F_{11,130} = 0.6368$, $P = 0.7945$), illustrating the unaltered circadian rhythm in feeder visits in Discordant mice. (*C*) Circadian rhythm in blood glucose of Discordant and Cre-negative control mice housed in constant darkness. CircWave analysis revealed significant rhythmicity in both genotypes, but no significant difference between genotypes. (*D*) Paired glucose tolerance tests of wild-type mice injected with standard or reduced glucose dose. Adult female mice housed in a 12-h light/12-h dark lighting cycle were fasted for 6 h before being injected with glucose (100%: 2.0 mg/gram body mass; 90%: 1.8 mg/gram body mass) in the middle of the light phase (Zeitgeber time 6–7). Comparison of repeated glucose tolerance tests on consecutive weeks showed that a 10% dosage difference did not significantly change the AUC (AUC: $F_{1,11} = 0.0004$, $P = 0.9853$). Asterisks indicate significant differences between dosages. Data are represented as mean ± SEM. Sample size is indicated at the base of each bar.

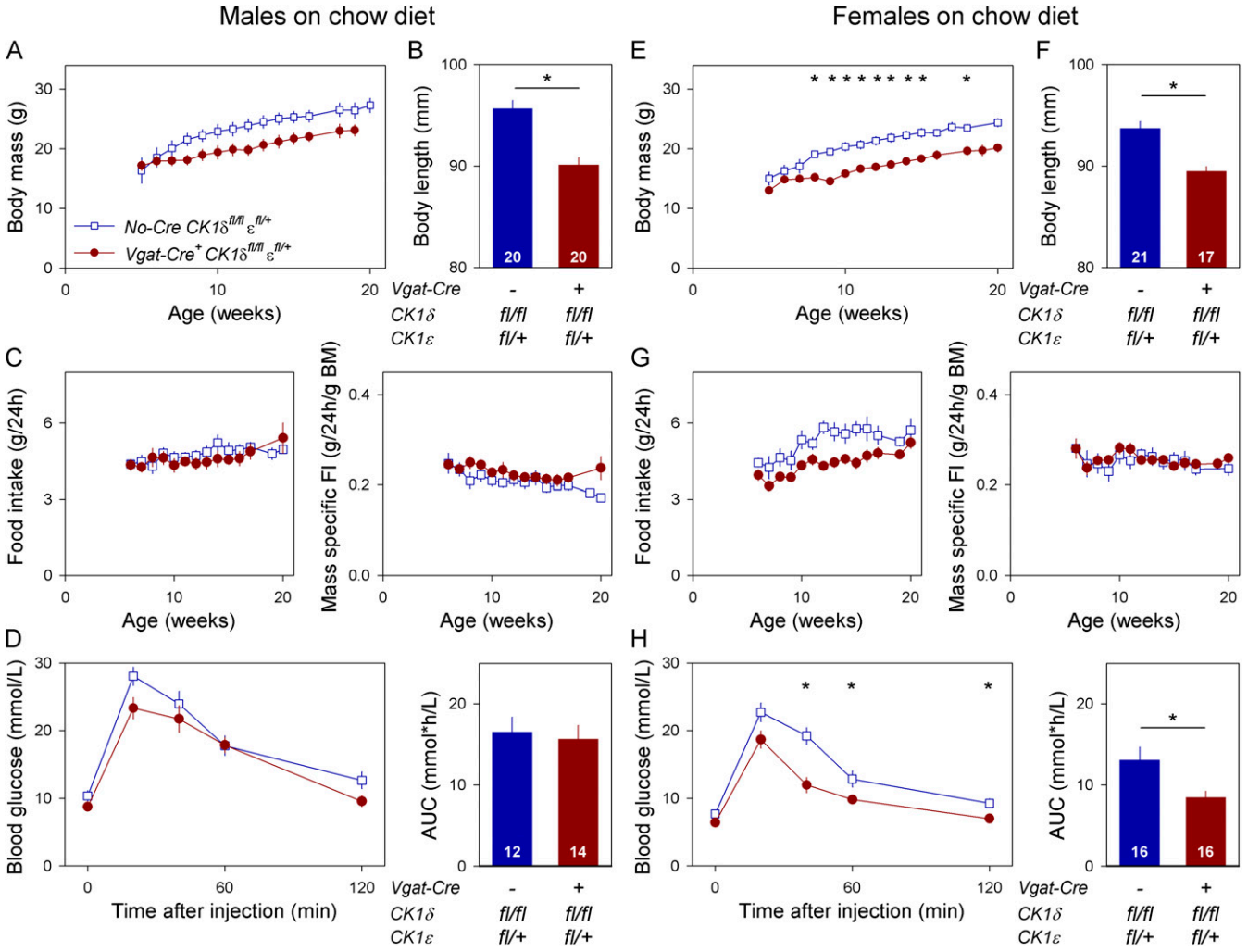

Fig. S5. Metabolic measurements of male (*Left*) and female (*Right*) Discordant mice (*Vgat-Cre*$^{+}$ *CK1δ*$^{fl/fl}$ *ε*$^{fl/+}$) and Cre-negative littermates (*No-Cre CK1δ*$^{fl/fl}$ *ε*$^{fl/+}$) fed regular chow diet and housed in constant darkness. (*A*) Weekly body mass measurements of 5- to 20-wk-old male mice. (*B*) Body length (distance from nose to base of tail) of adult male mice. (*C*) Food intake (*Left*) and mass-specific food intake (FI) (*Right*) of 5- to 20-wk-old male mice. (*D*) Glucose tolerance tests of adult male mice performed in the middle of the rest phase following a 6-h fast. (*E*) Weekly body mass measurements of 5- to 20-wk-old female mice. (*F*) Body length (distance from nose to base of tail) of adult female mice. (*G*) Food intake (*Left*) and mass-specific food intake (*Right*) of 5- to 20-wk-old female mice. Although absolute food intake differed between genotypes ($F_{1,10.5} = 619.4$, $P < 0.0001$), this difference disappeared when food intake was expressed relative to body mass ($F_{1,10.7} = 0.1357$, $P = 0.7198$). (*H*) Glucose tolerance tests of adult female mice performed in the middle of the rest phase following a 6-h fast. Data are represented as mean ± SEM. Sample size per genotype is indicated at the base of each bar. Asterisks indicate significant differences between genotypes.

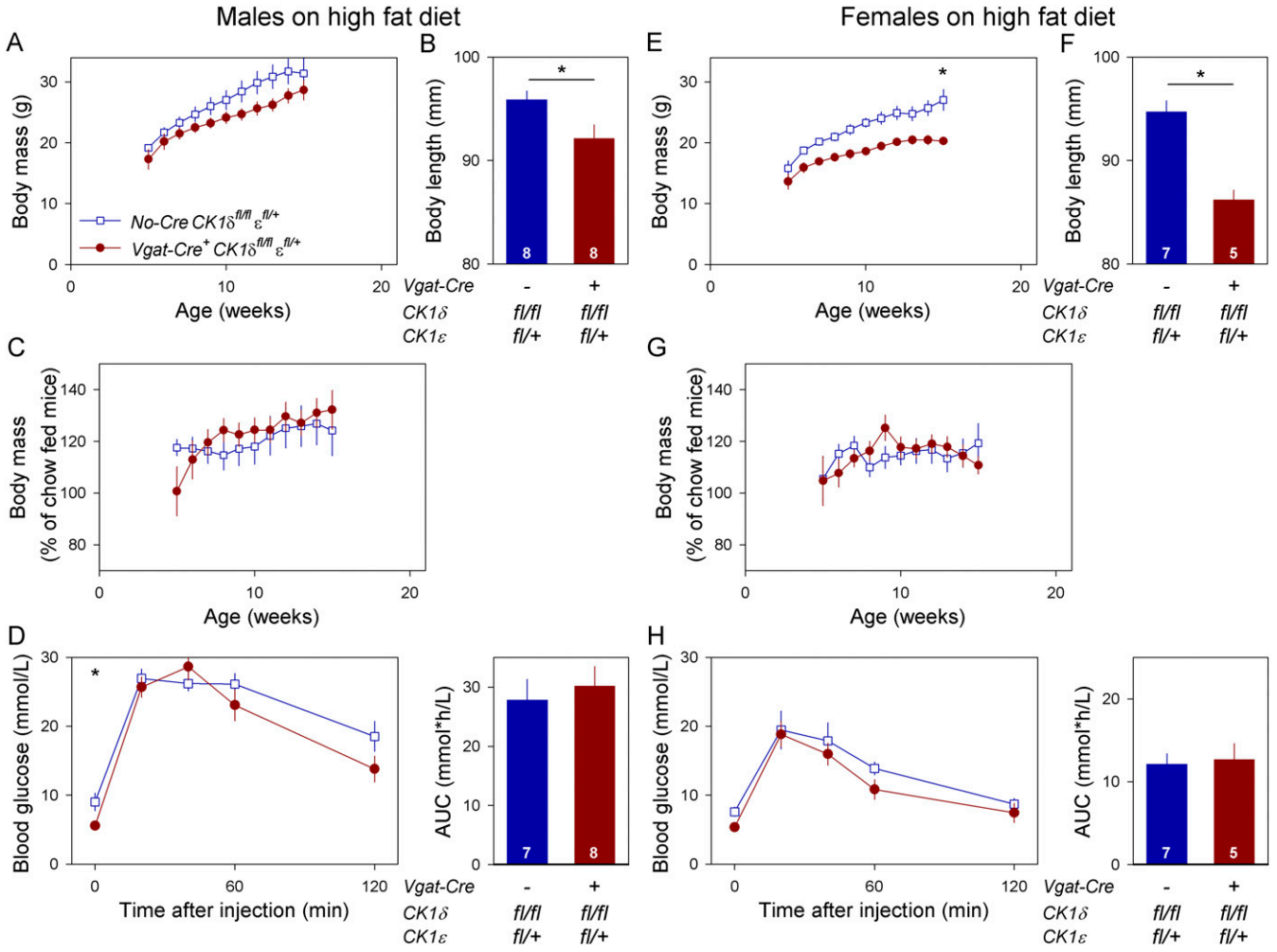

Fig. S6. Metabolic measurements of male (*Left*) and female (*Right*) Discordant mice (*Vgat-Cre*$^{+}$ *CK1δ*$^{fl/fl}$ *ε*$^{fl/+}$) and Cre-negative littermates (*No-Cre CK1δ*$^{fl/fl}$ *ε*$^{fl/+}$) on high-fat diet housed in constant darkness. (*A*) Weekly body mass measurements of 5- to 16-wk-old male mice. (*B*) Body length (distance from nose to base of tail) of adult male mice. (*C*) Body mass relative to chow-fed mice (Fig. S5*A*) of 5- to 16-wk-old male mice. (*D*) Glucose tolerance tests of adult male mice performed in the middle of the rest phase following an 18 circadian-hour fast. (*E*) Weekly body mass measurements of 5- to 16-wk-old female mice. (*F*) Body length (distance from nose to base of tail) of adult female mice. (*G*) Body mass relative to chow-fed mice (Fig. S5*E*) of 5- to 16-wk-old female mice. (*H*) Glucose tolerance tests of adult female mice performed in the middle of the rest phase following an 18 circadian-hour fast. Data are represented as mean ± SEM. Sample size per genotype is indicated at the base of each bar. Asterisks indicate significant differences between genotypes.

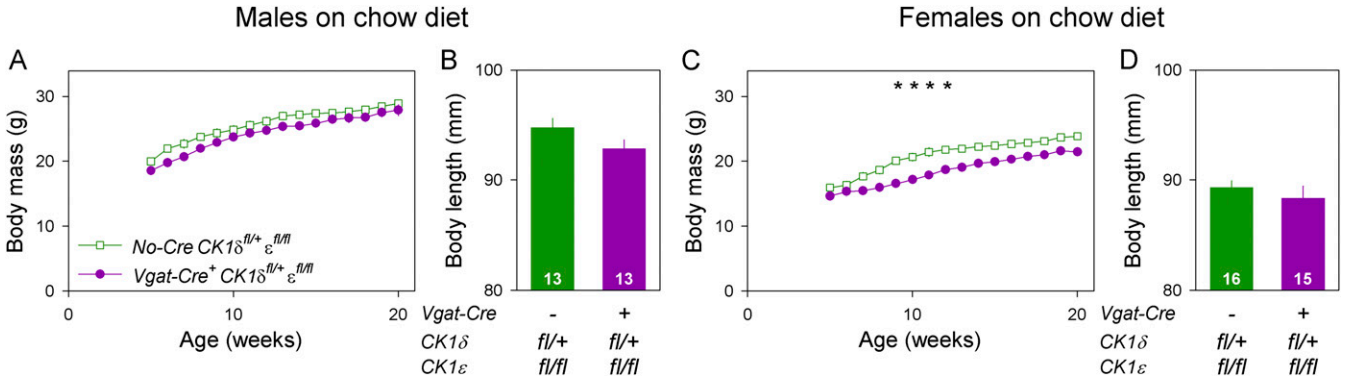

Fig. S7. Metabolic measurements of male (*Left*) and female (*Right*) mice with deletions of one allele of *CK1δ* and both alleles of *CK1ε* in GABAergic neurons (*Vgat-Cre*$^{+}$ *CK1δ*$^{fl/+}$ *ε*$^{fl/fl}$) and their Cre-negative littermates (*No-Cre CK1δ*$^{fl/+}$ *ε*$^{fl/fl}$) on chow diet housed in constant darkness. (*A*) Weekly body mass measurements of 5- to 20-wk-old male mice. (*B*) Body length (distance from nose to base of tail) of adult male mice. (*C*) Weekly body mass measurements of 5- to 20-wk-old female mice. (*D*) Body length (distance from nose to base of tail) of adult female mice. Data are represented as mean ± SEM. Sample size per genotype is indicated at the base of each bar. Asterisks indicate significant differences between genotypes.

Table S1. Statistical outcomes of in vivo peripheral PER2::LUC bioluminescence rhythmicity analysis of Discordant and Cre-negative control mice housed in constant darkness

	Cre-negative control (*No-Cre CK1δ$^{fl/fl}$ ε$^{fl/+}$*)		Discordant mice (*Vgat-Cre^{+} CK1δ$^{fl/fl}$ ε$^{fl/+}$*)		
Tissue	Peak phase (CT ± SEM)	Rayleigh test	Peak phase (CT ± SEM)	Rayleigh test	Watson U^2 test
Submandibular gland	17.7 ± 0.3 h	$Z_9 = 8.68$, $P < 0.001$	11.1 ± 0.9 h	$Z_8 = 5.46$, $P = 0.002$	$U^2 = 0.391$, $P < 0.005$
Liver	18.8 ± 0.2 h	$Z_9 = 8.82$, $P < 0.001$	12.9 ± 0.8 h	$Z_8 = 5.82$, $P = 0.008$	$U^2 = 0.499$, $P < 0.005$
Left kidney	17.6 ± 0.5 h	$Z_7 = 6.39$, $P < 0.001$	13.0 ± 0.8 h	$Z_7 = 5.43$, $P = 0.001$	$U^2 = 0.499$, $P < 0.005$
Right kidney	17.2 ± 0.8 h	$Z_7 = 5.41$, $P = 0.001$	13.0 ± 0.8 h	$Z_7 = 5.43$, $P = 0.001$	$U^2 = 0.458$, $P < 0.005$

CT, circadian time. Related to Fig. 2.

Table S2. Statistical outcomes of body temperature, energy expenditure, mass-specific energy expenditure, and respiratory quotient comparisons of Discordant and Cre-negative control mice housed in constant darkness

	Comparison between rest and active phase			
Measurement	Cre-negative control (*No-Cre CK1δ$^{fl/fl}$ ε$^{fl/+}$*)	Discordant mice (*Vgat-Cre^{+} CK1δ$^{fl/fl}$ ε$^{fl/+}$*)	Amplitude differences between genotypes	Differences in daily average between genotypes
Males				
Body temperature	$F_{1,7} = 68.44$, $P < 0.0001$	$F_{1,5} = 504.6$, $P < 0.0001$	$F_{1,12} = 8.958$, $P = 0.0112$	$F_{1,12} = 9.439$, $P = 0.0097$
Energy expenditure	$F_{1,7} = 126.1$, $P < 0.0001$	$F_{1,5} = 115.0$, $P < 0.0001$	$F_{1,12} = 7.553$, $P = 0.0177$	$F_{1,12} = 0.4058$, $P = 0.5361$
Mass-specific EE	$F_{1,7} = 113.7$, $P < 0.0001$	$F_{1,5} = 280.5$, $P < 0.0001$	$F_{1,12} = 19.79$, $P = 0.0008$	$F_{1,12} = 1.315$, $P = 0.2738$
Respiratory quotient	$F_{1,7} = 7.778$, $P = 0.0270$	$F_{1,5} = 28.14$, $P = 0.0032$	$F_{1,12} = 2.470$, $P = 0.1420$	$F_{1,12} = 1.156$, $P = 0.3034$
Females				
Body temperature	$F_{1,6} = 126.2$, $P < 0.0001$	$F_{1,5} = 59.28$, $P = 0.0006$	$F_{1,11} = 0.0035$, $P = 0.9539$	$F_{1,11} = 0.0287$, $P = 0.8686$
Energy expenditure	$F_{1,6} = 13.50$, $P = 0.0104$	$F_{1,5} = 34.42$, $P = 0.0020$	$F_{1,11} = 1.422$, $P = 0.2582$	$F_{1,11} = 0.0001$, $P = 0.9918$
Mass-specific EE	$F_{1,6} = 12.77$, $P = 0.0117$	$F_{1,5} = 49.63$, $P = 0.0009$	$F_{1,11} = 3.165$, $P = 0.1029$	$F_{1,11} = 1.832$, $P = 0.2031$
Respiratory quotient	$F_{1,6} = 5.274$, $P = 0.0614$	$F_{1,5} = 17.90$, $P = 0.0082$	$F_{1,11} = 0.1321$, $P = 0.7231$	$F_{1,11} = 2.663$, $P = 0.1321$

Related to Fig. 3.

Table S3. Statistical outcomes of in vivo peripheral PER2::LUC bioluminescence rhythmicity analysis of Discordant and Cre-negative control mice housed in a 2-h light/23.5-h dark lighting cycle

	Cre-negative control (*No-Cre CK1δ$^{fl/fl}$ ε$^{fl/+}$*)		Discordant mice (*Vgat-Cre^{+} CK1δ$^{fl/fl}$ ε$^{fl/+}$*)		
Tissue	Peak phase (CT ± SEM)	Rayleigh test	Peak phase (CT ± SEM)	Rayleigh test	Watson U^2 test
Submandibular gland	15.6 ± 0.3 h	$Z_6 = 5.78$, $P < 0.001$	16.1 ± 0.9 h	$Z_6 = 4.60$, $P = 0.004$	$U^2 = 0.16$, $0.2 > P < 0.1$
Liver	16.6 ± 0.3 h	$Z_6 = 5.83$, $P < 0.001$	17.1 ± 0.5 h	$Z_6 = 5.48$, $P < 0.001$	$U^2 = 0.06$, $P > 0.5$
Left kidney	15.7 ± 0.8 h	$Z_6 = 4.69$, $P = 0.004$	16.8 ± 0.4 h	$Z_6 = 5.69$, $P < 0.001$	$U^2 = 0.042$, $P > 0.5$
Right kidney	17.0 ± 0.7 h	$Z_6 = 5.14$, $P = 0.002$	16.4 ± 0.3 h	$Z_6 = 5.77$, $P < 0.001$	$U^2 = 0.097$, $0.5 > P > 0.2$

CT, circadian time. Related to Fig. 6.